

# CHALMERS



## Modeling and simulation of rotary bell spray atomizers in automotive paint shops

BJÖRN ANDERSSON

Department of Applied Mechanics  
*Division of Fluid Dynamics*  
CHALMERS UNIVERSITY OF TECHNOLOGY  
Gothenburg, Sweden 2013



THESIS FOR THE DEGREE OF DOCTOR OF PHILOSOPHY  
IN  
THERMO AND FLUID DYNAMICS

Modeling and simulation of rotary bell spray atomizers in  
automotive paint shops

BJÖRN ANDERSSON

Department of Applied Mechanics  
*Division of Fluid Dynamics*  
CHALMERS UNIVERSITY OF TECHNOLOGY  
Gothenburg, Sweden 2013

Modeling and simulation of rotary bell spray atomizers in automotive paint shops  
BJÖRN ANDERSSON  
ISBN 978-91-7385-940-0

© BJÖRN ANDERSSON, 2013

Doktorsavhandlingar vid Chalmers tekniska högskola  
Ny serie nr. 3621  
ISSN 0346-718X  
Department of Applied Mechanics  
Division of Fluid Dynamics  
Chalmers University of Technology  
SE-412 96 Gothenburg  
Sweden  
Telephone: +46 (0)31-772 1000

Chalmers Reproservice  
Gothenburg, Sweden 2013

# Modeling and simulation of rotary bell spray atomizers in automotive paint shops

Thesis for the degree of Doctor of Philosophy in Thermo and Fluid Dynamics

BJÖRN ANDERSSON

Department of Applied Mechanics, Division of Fluid Dynamics  
Chalmers University of Technology

and

Department of Computational Engineering and Design  
Fraunhofer-Chalmers Research Centre for Industrial Mathematics

## ABSTRACT

The paint and surface treatment processes in automotive paint shops are characterized by multiphase and free surface flows, multiphysics interactions, multiscale phenomena, and large moving geometries. The current version of the software for simulation of spray painting developed at the Fraunhofer-Chalmers Centre relies on measurements of droplet size distributions and velocity profiles below the applicator that can be used as input to the simulations. This thesis discusses techniques that can be used to reduce the need for costly and complicated measurements by performing detailed simulations instead.

Surface tension plays an important role during breakup as it acts to stabilize the droplets. On the small scales of droplets from 1-100  $\mu m$  in diameter it is a strong force yet localized to the interface between the droplet and the surrounding medium. It is therefore crucial to have control over the interface and to this end a novel method for reconstructing the interface of the droplet is proposed. The method relies on approximation by Radial Basis Functions using a technique that enables the omission of small length scale structures in order to obtain a smooth representation that is suitable for numerical discretization.

Droplet size distributions have been simulated with the Taylor Analogy Breakup model. A modification taking the large viscosity of the paint into account is introduced to the model and it is applied to the case of rotary bell spray painting commonly used in automotive industry. Results show that the model is able to capture the overall shape of the size distributions, as well as the local spatial dependencies on the size distributions where large droplets are typically found further away from the center.

By gaining a better understanding of the physical conditions close to the paint applicator the need for costly and complicated measurements is decreased. Having access to tools for fast and efficient simulation of the spray painting processes would be advantageous, since such tools can contribute to reduce the time required for introduction of new models, reduce the cycle time, reduce the environmental impact, and increase quality.

Keywords: spray painting, breakup, atomization, surface tension, computational fluid dynamics, coating, multiphase flow



## ACKNOWLEDGMENTS

I wish to extend my personal thanks to

- my boss Assoc. Prof. Fredrik Edelvik and FCC's director Dr. Johan S. Carlsson for giving me the opportunity to study the topic of breakup in great detail.
- my supervisors Prof. Lars Davidson, Assoc. Prof. Valeri Golovitchev, and Dr. Andreas Mark for their support and encouragement.
- Dr. Stefan Jakobsson for always allowing me some of his time.
- my colleagues at FCC, in particular at the department of Computational Engineering and Design: Lic. Anders Ålund, Dr. Andreas Mark, Anton Berce, Dr. Christoffer Cromvik, Cornelia Jareteg, Elin Solberg, Dr. Johan Nyström, Martin Svensson, Niklas Karlsson, Dr. Pekka Røyttä, Dr. Stefan Jakobsson, and Dr. Tomas Johnson. In addition, support from our previous colleagues Erik Svenning, Dr. Robert Rundqvist, and Dr. Robert Sandboge is acknowledged.
- Prof. Bernhard Mehlig of the physics department at the University of Gothenburg for all his support in every aspect and for introducing me to the subject of particles in turbulent flows.
- my parents and the family of my brother for their support and for allowing me a place to regain energy.

This work has been conducted within the Virtual Paint Shop project with the partners Volvo Cars, SAAB Automobile, Scania, AB Volvo, Swerea IVF, Konga Bruk and General Motors NA. It was supported in part by the Swedish Governmental Agency for Innovation Systems, VINNOVA, through the FFI Sustainable Production Technology Program and in part by the Sustainable Production Initiative and the Production Area of Advance at Chalmers. Some of the simulations were performed on resources at Chalmers Centre for Computational Science and Engineering (C3SE) provided by the Swedish National Infrastructure for Computing (SNIC). The support is gratefully acknowledged.

Björn Andersson  
Göteborg, November 2013



## LIST OF PAPERS

- Paper I** A. Mark, B. Andersson, S. Tafuri, K. Engström, H. Söröd, F. Edelvik, and J. S. Carlson. Simulation of Electrostatic Rotary Bell Spray Painting in Automotive Paint Shops. *Atomization and Sprays* **23.1** (2013), 25–45.
- Paper II** B. Andersson, S. Jakobsson, A. Mark, F. Edelvik, and L. Davidson. “Modeling Surface Tension in SPH by Interface Reconstruction using Radial Basis Functions”. *Proceedings of the 5<sup>th</sup> International SPHERIC Workshop*. Ed. by B.D. Rogers. Manchester (U.K.), June 2010, pp. 7–14.
- Paper III** B. Andersson, V. Golovitchev, S. Jakobsson, A. Mark, F. Edelvik, L. Davidson, and J. S. Carlson. A Modified TAB Model for Simulation of Atomization in Rotary Bell Spray Painting. *Journal of Mechanical Engineering and Automation* **3.2** (2013), 54–61.
- Paper IV** B. Andersson, A. Ålund, A. Mark, and F. Edelvik. *MPI-Parallelization of a Structured Grid CFD Solver including an Integrated Octree Grid Generator*. Tech. rep. 2013-05. Chalmers University of Technology, Sept. 2013.
- Paper V** B. Andersson, S. Jakobsson, A. Mark, F. Edelvik, and L. Davidson. “Modeling Surface Tension by Interface Reconstruction using Radial Basis Functions”. Submitted to *Journal of Multiphase Flow*.
- Paper VI** B. Andersson, A. Mark, L. Davidson, F. Edelvik, and J. Carlson. “Modeling and Simulation of Droplet Breakup in Automotive Spray Painting”. To be submitted for journal publication.

## DISTRIBUTION OF WORK

### Paper I

Mark derived the numerical discretization of the solvers, performed the simulations and validated the results. The solvers were implemented by Mark and Andersson, paint thickness integration by Tafuri. The graphical user interface and supporting functionality were implemented and adapted by Tafuri and Engström. The measurements were supervised by Söröd, Mark, and Andersson. The manuscript was prepared by Edelvik and Mark. Andersson, Tafuri, Engström, Edelvik, and Carlson contributed with discussion of ideas and reviewing of the manuscript.

### Paper II

The idea was jointly sketched by Andersson and Jakobsson, where Jakobsson provided expertise on radial basis functions as well as a C++ implementation thereof. The proposed method was derived, implemented and validated by Andersson. Mark and Andersson implemented and adapted the underlying CFD solver. Andersson prepared the manuscript and Mark, Edelvik, and Davidson contributed with discussion of ideas and reviewing of the manuscript.

### Paper III

The idea of applying the TAB model was initiated by Golovitchev. The modification of the model, the implementation, running and validation of simulations were performed by Andersson, who also prepared the manuscript and took part in implementing and adapting the CFD solver together with Mark. Jakobsson provided advice on the optimization of model parameters. Golovitchev, Jakobsson, Mark, Edelvik, Davidson, and Carlson contributed with discussion of ideas and reviewing of the manuscript.

### Paper IV

Andersson performed the MPI-parallelization of the existing serial solver implemented by Mark and Andersson. Ålund and Mark provided advice on MPI library usage. Andersson and Ålund ran the software and analyzed the performance. The manuscript was prepared by Andersson and the work was reviewed by Edelvik.

### Paper V

The idea was jointly sketched by Andersson and Jakobsson, where Jakobsson provided expertise on radial basis functions as well as a C++ implementation thereof. The proposed method was derived, implemented and validated by Andersson. Mark and Andersson implemented and adapted the underlying CFD solver. Andersson prepared the manuscript and Mark, Edelvik, and Davidson contributed with discussion of ideas and reviewing of the manuscript.

## Paper VI

Andersson modeled the setup with advice from Mark, ran the simulations and validated the results, and implemented the breakup model. The CFD solver was implemented and adapted by Mark and Andersson. Andersson prepared the manuscript, and Mark, Edelvik, Davidson, and Carlson contributed with discussion of ideas and reviewing of the manuscript.



# CONTENTS

<b>Abstract</b>	<b>iii</b>
<b>Acknowledgments</b>	<b>v</b>
<b>List of papers</b>	<b>vii</b>
<b>Distribution of work</b>	<b>viii</b>
<b>Contents</b>	<b>xi</b>
<b>I Extended Summary</b>	<b>1</b>
<b>1 Introduction</b>	<b>3</b>
<b>2 Breakup: Important concepts and numerical modeling</b>	<b>7</b>
2.1 Characterization of breakup . . . . .	7
2.1.1 Primary breakup . . . . .	7
2.1.2 Secondary breakup . . . . .	7
2.2 Surface tension . . . . .	9
2.2.1 Surface tension discretization . . . . .	9
2.3 Stability criterion . . . . .	11
2.4 Numerical modeling . . . . .	12
2.4.1 Instability theory . . . . .	12
2.4.2 TAB model . . . . .	13
<b>3 Measurement techniques</b>	<b>15</b>
3.1 Particle Image Velocimetry (PIV) . . . . .	15
3.2 Phase Doppler Anemometry (PDA) . . . . .	16
3.3 Laser diffraction . . . . .	16
3.4 Shadowgraph . . . . .	18
<b>4 High performance computing</b>	<b>21</b>
4.1 Parallelization . . . . .	21
4.1.1 Shared memory parallelization . . . . .	21
4.1.2 Message passing . . . . .	22
4.2 Accelerators . . . . .	24
<b>5 Summary of appended papers</b>	<b>27</b>
5.1 Paper I — Simulation of Electrostatic Rotary Bell Spray Painting in Automotive Paint Shops . . . . .	27
5.2 Paper II — Modeling Surface Tension in SPH by Interface Reconstruction using Radial Basis Functions . . . . .	27

5.3	Paper III — A Modified TAB Model for Simulation of Atomization in Rotary Bell Spray Painting . . . . .	28
5.4	Paper IV — MPI-Parallelization of a Structured Grid CFD Solver including an Integrated Octree Grid Generator . . . . .	28
5.5	Paper V — Modeling Surface Tension by Interface Reconstruction using Radial Basis Functions . . . . .	29
5.6	Paper VI — Modeling and Simulation of Droplet Breakup in Automotive Spray Painting . . . . .	29
<b>6</b>	<b>Summary and future work</b>	<b>31</b>
	<b>References</b>	<b>33</b>
<b>II</b>	<b>Appended Papers I–VI</b>	<b>37</b>

Part I  
Extended Summary



# 1 Introduction

The paint and surface treatment processes in automotive paint shops are characterized by multiphase and free surface flows, multiphysics interactions, multiscale phenomena, and large moving geometries. This poses great challenges for mathematical modeling and simulation. The current situation in the automotive industry is therefore to rely on individual experience and physical validation for improving these processes. Having access to tools that incorporate the flexibility of robotic path planning with fast and efficient simulation of the processes would be advantageous, since such tools can contribute to reduce the time required for introduction of new models, reduce the cycle time, reduce the environmental impact, and increase quality.

A framework that allows for accurate simulations of spray painting of a car in just a few hours on a standard computer has been developed at the Fraunhofer-Chalmers Centre. To achieve this, novel algorithms are developed for coupled simulations of air flow, electromagnetic fields, and charged paint droplets. Particularly important for the computational efficiency is the Navier-Stokes solver. Unique, immersed boundary methods are used to model the presence of objects in the fluid and they are combined with an adaptive Cartesian octree grid [31, 30]. This enables modeling of moving objects at virtually no additional computational cost, and greatly simplifies preprocessing by avoiding the cumbersome generation of a body-conforming mesh. Figure 1.1 shows a snapshot of a robot painting a car door, and Fig. 1.2 shows the painting of a full Volvo V60.

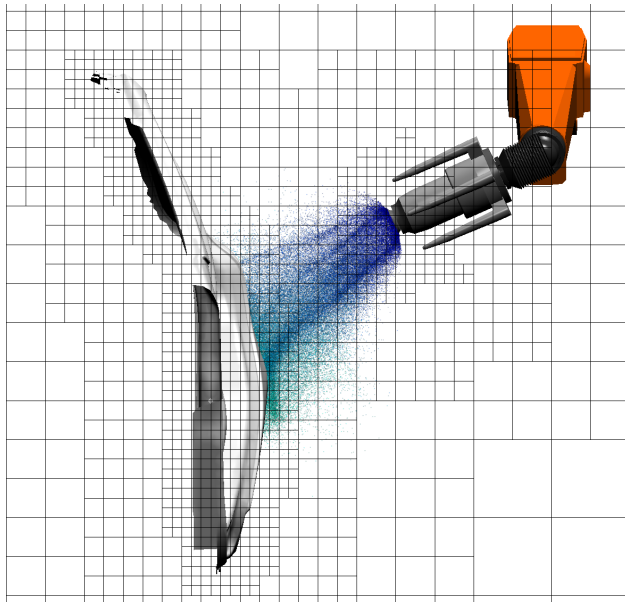


Figure 1.1: Virtual spray painting of a car door in the IPS Virtual Paint software. CAD geometry courtesy of Volvo Car Corporation.

The focus is on spray painting with the electrostatic rotary bell sprayer (ERBS) technique. Paint is injected at the center of a rotating bell; the paint forms a film on the bottom side of the bell and is atomized at the edge. The droplets may be charged electrostatically and driven toward the target both by shaping air surrounding the rotating bell and by a potential difference in the order of 50–100 kV between paint applicator and target. A close-up of an active bell spraying towards a plate is shown in Fig. 1.3, and the geometry of the actual bell can be seen in Fig. 1.4.

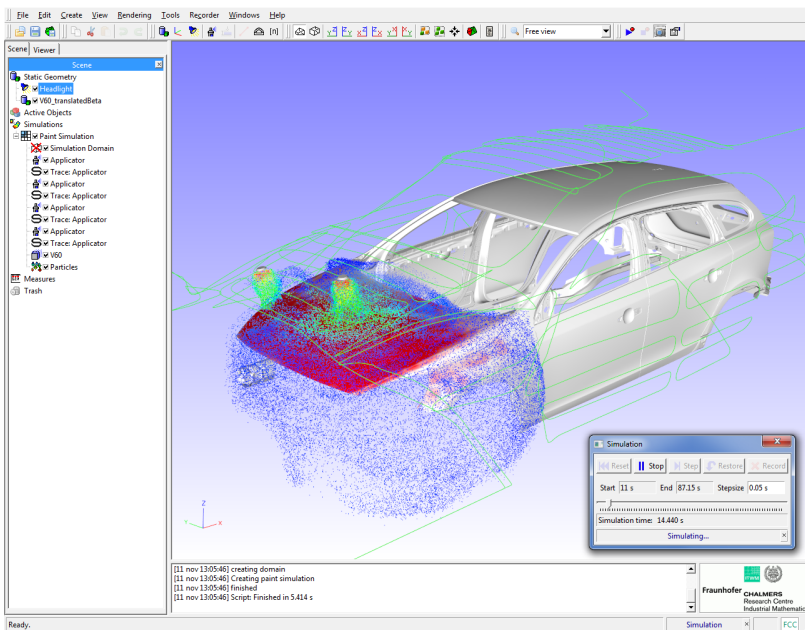
A few attempts to simulate the complex process by Ellwood *et al.* [16], Huang *et al.* [20], Im *et al.* [22], Viti *et al.* [52, 53], and Ye *et al.* [57] can be found in the literature. In particular, Domnick *et al.* [15, 14] have made extensive modeling work for wet paint as well as for powder coating devices. A systematic validation for realistic geometries is missing and another major drawback with earlier approaches is that the simulation times are prohibitively long for the tools to be industrially useful. This is partly because the simulation methods do not handle moving geometries in an efficient way.

When spraying with a rotary bell sprayer paint is injected at the center of a rotating bell as shown in Fig. 1.4. Due to the large rotational speed of the bell a paint film is formed on the bottom side of the bell. At the edge of the bell the paint falls off into the surrounding air, and is rapidly atomized by the large force caused by aerodynamic drag. In the current version of the FCC software IPS Virtual Paint [23] the atomization step is not simulated but instead measurements of droplet size and velocity distributions close to the bell are required as input. These measurements are costly and requires special equipment to perform. In addition, creating initial conditions for the spray simulation involve some manual tuning of the parameters in the model to match the numerical solution to the measured fields. This thesis aims to create a better understanding of the flow conditions and physical processes active in the region close to the bell. If a good understanding is gained this can be used to create efficient numerical tools for simulating these processes, and to better utilize the capabilities of the equipment. A large part of what is happening close to the bell is governed by the interaction of the paint and surrounding air. The paint is injected in the tangential direction of the bell edge, which is orthogonal to the direction towards the object to be painted. The paint therefore has to be re-directed towards the object, and this is done by a combination of electrostatic forces and aerodynamic drag caused by the injection of the so-called shape air. As the paint velocity vector is turned by approximately 90° towards the paint target the paint droplets break and form smaller droplets. How fast this breakup process is, and how large the resulting droplets are have a large impact on how the spray behaves.

The droplet size distribution determines the characteristics of the spray and how it reacts to the external forces applied by the air and the electrostatic field: large droplets tend to travel in straight lines and small droplets follow the force field closely. The behavior is characterized by the Stokes number that relates the response time of the particle to the timescale on which the field changes on. The particle response time is a function of its size, and also its electric charge if a voltage is applied to the applicator. The response time also scales differently for the fluid and the electromagnetic interaction. It is therefore important to have good knowledge on the distribution of droplet sizes present in the spray in order to be able to perform spray painting simulations with high accuracy. If a better understanding on how the process parameters affect the paint film distribution is



(a) Actual painting



(b) Virtual painting

Figure 1.2: Painting of a Volvo V60 with several robots spraying simultaneously. Photograph and CAD geometry courtesy of Volvo Car Corporation.

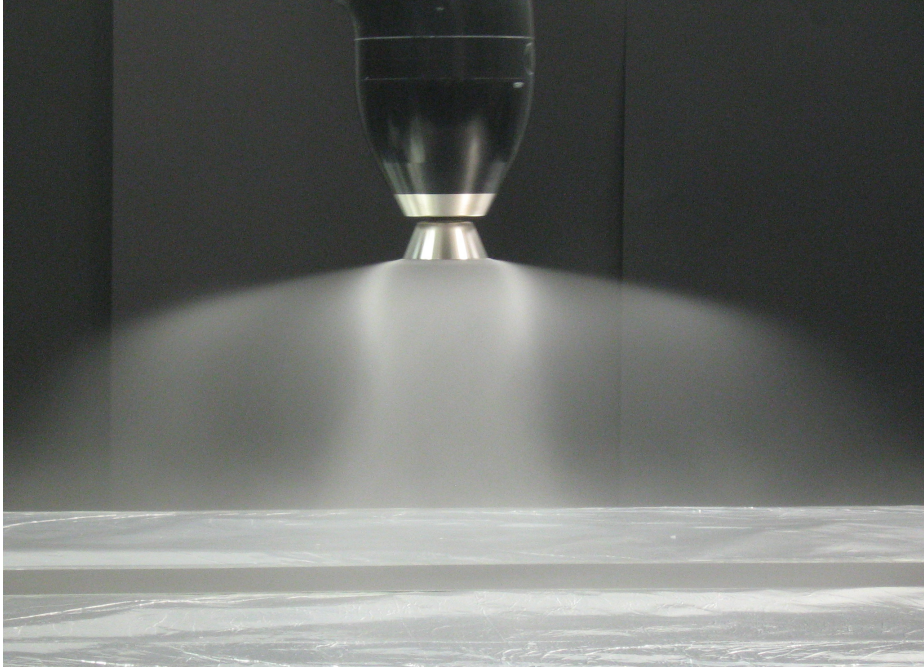


Figure 1.3: Photograph of rotary bell spraying towards a target. The actual bell is the cone shaped part at the tip of the applicator head. Photograph courtesy of Swerea IVF.

gained it can be used in an optimization loop to tune the result of the painting to have a better visual appearance, be more cost effective, and to be more environmentally friendly.



Figure 1.4: Geometry of a bell, shown from below. The outer diameter of the bell is 65 mm. The paint is injected in the middle and forms a film on the bottom side. The bell spins rapidly, with up to 50 000 revolutions per minute, and the paint is forced towards the edge where it enters the air and is atomized.

# 2 Breakup: Important concepts and numerical modeling

A large part of the work has been focused on understanding and modeling the breakup of the paint droplets. This section gives an overview of the area.

## 2.1 Characterization of breakup

In order to reduce the costly and cumbersome size distribution measurements, the idea is to simulate the break-up of paint into droplets. By studying the region closest to the bell edge where the breakup is taking place the atomization process can be characterized into two main components: Primary and secondary breakup. A snapshot of paint breaking up is shown in Fig. 2.1 in which filaments of paint can be seen emanating from the edge of the bell. These filaments are formed by serrations at the bell edge that act as small channels for the paint, forcing it into the shape of evenly spaced fingers. The filaments are distorted by instabilities driven by the relative velocity to the air, and once the distortion is large enough, fragments break off. The fragments typically break further before reaching a stable size. This is called the secondary breakup.

### 2.1.1 Primary breakup

The primary breakup is not extensively treated in this thesis. In paper III [4] the size distribution of the fragments of the primary breakup is modeled with a log-normal distribution with fragment sizes with mean and standard deviation equal to 100 and 50  $\mu m$ , respectively. The speed of the fragments also needs modeling as it is reasonable to assume that at least some of the filaments' relative velocity to the air is lost before splitting into fragments. In the paper the velocity of the fragments is modeled as a uniform distribution varying between the full tangential speed of the bell edge down to half of it. In other words, up to half the velocity is lost upon completion of the primary breakup, but only a minority of the fragments lose this much.

Experimental treatment of the primary breakup in isolation is of course difficult, as one cannot stop the fragments from undergoing the secondary breakup. High speed imaging is however a possibility as shown in Fig. 2.1. By taking multiple such pictures with a small time separation it would be possible to estimate the speed of the filaments. The wavelength and development of the instabilities would also be possible to measure. Broken fragments might be possible to capture with the camera so that they could be measured, but this has proved to be difficult in practice.

### 2.1.2 Secondary breakup

The secondary breakup is targeted in paper III [4] where the Taylor Analogy Breakup (TAB) model [38] is applied to the spray paint application. In the model droplets are modeled as harmonic oscillators, driven by their relative speed to the air. By adding

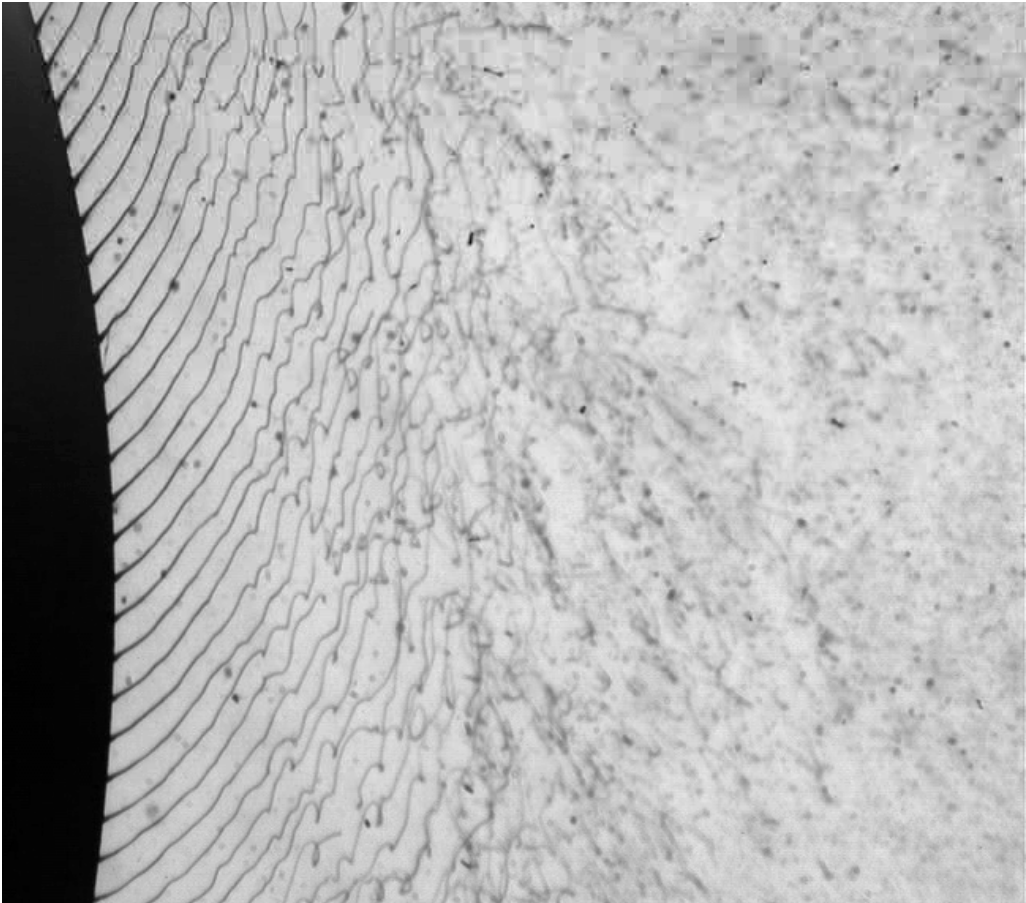


Figure 2.1: Snapshot of paint breaking up. The bell edge is visible to the left and the paint enters the air as evenly spaced filaments. The bell spins giving the part of the edge shown a velocity directed downwards, creating the spiraling pattern of the filaments. After a few millimeters the filaments are distorted to the point where they break, forming non-spherical droplets breaking up further before forming stable droplets. Photograph courtesy of Swerea IVF.

coefficients to the expression for the drag force, restoring force, and the viscous force, the size distribution can be simulated by tuning the coefficients so that the results match the measurements. The TAB model does not, however, give much information about the qualitative breakup process as it is more complicated than what can be modeled by a harmonic oscillator. The reader is referred to [41] for an overview of the different breakup modes active in different regions of the phase space.

Experimental results for the secondary breakup are possible to extract, at least in the sense of the final result. The difficulty here is instead the initial conditions, that of course are the final result of the primary breakup. The secondary breakup is to some extent independent on the primary one, however, as droplets will continue to break until they are stable. It is probably reasonable to expect that second generation child droplets have lost the memory of the size and shape of the grand parent droplet. First generation child droplets may on the other hand have some heritage left, and the question that needs to be answered is how many generations of child droplets that are produced on average.

## 2.2 Surface tension

Surface tension is an important concept in breakup simulations as it is a stabilizing force acting on the droplet to prevent breakup. It acts on the interface of the droplet to the air with a magnitude that is proportional to the mean curvature of the interface,

$$\mathbf{F}_s = -\sigma \frac{\kappa_1 + \kappa_2}{2} \hat{\mathbf{n}}, \quad (2.1)$$

where  $\sigma$  is the surface tension coefficient,  $\kappa_1$  and  $\kappa_2$  are the two principal curvatures, and  $\hat{\mathbf{n}}$  is the outward pointing normal of the interface. For a sphere the mean curvature is the inverse of its radius so that

$$\mathbf{F}_s = -\frac{\sigma}{R} \hat{\mathbf{n}}. \quad (2.2)$$

The force therefore grows as the radius of the droplet becomes smaller, and at some point it becomes the dominant force.

### 2.2.1 Surface tension discretization

If seen on an atomistic scale the surface tension acts on a thickness of a few atomic layers [54], but in practice with a realistic resolution the force can be seen to act on a two-dimensional manifold embedded in three dimensions. To overcome this problem and to convert it into a volume force acting in a narrow band, Brackbill *et al.* derived [8] the Continuum Surface Force (CSF) approach that enables the force to be applied to the neighboring cells to the interface in a computational code.

Even though the discretization of the force is converted to act as a localized volume force, stability problems can arise for smaller droplets because of the scaling shown in Eq. 2.2. Papers II and V [6, 5] describe a new method to discretize the force that is in some sense independent of the grid that the Navier-Stokes equations are discretized on. In this way a smoother discretization is enabled that proved to increase the stability of the numerical simulations. The method relies on an implicit surface reconstructed by

means of Radial Basis Functions [55, 10, 11] with the approximation feature described in [24]. This gives a smooth reconstructed interface suitable for evaluating the surface tension. By using relations for implicit surfaces derived by Goldman [18] the following expression is obtained for the surface tension force

$$\mathbf{F}_s = \sigma \kappa \hat{\mathbf{n}}, \quad (2.3)$$

with

$$\kappa = \frac{\nabla C^T H(C) \nabla C - |\nabla C|^2 \text{Trace}(H(C))}{(d-1) |\nabla C|^3}, \quad (2.4)$$

where  $\sigma$  is the surface tension coefficient,  $\kappa$  is the mean curvature of the interface,  $\hat{\mathbf{n}}$  is the interface unit normal,  $C$  is the implicit surface,  $H(\cdot)$  is the Hessian operator, and  $d$  is the number of spatial dimensions. Figure 2.2 shows an example of the surface tension force evaluated in the corner of an initially square droplet, together with a reference implementation of the standard CSF method [8]. It is clearly seen that the new method gives a surface tension discretization that is more favorable in numerical simulations.

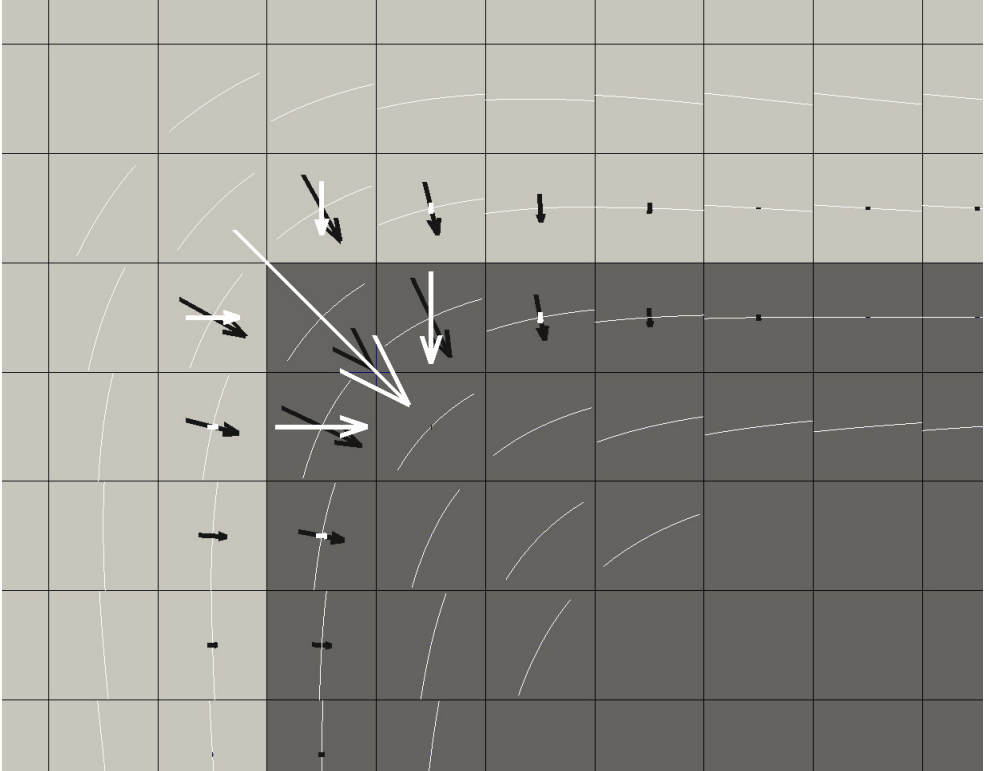


Figure 2.2: Surface tension force evaluated at an interface. New method (black arrows) and the standard CSF method (white arrows). Level curves of the implicit surface are also shown going through the centers of the computational cells.

## 2.3 Stability criterion

The droplet stability level can be expressed by the dimensionless Weber number,

$$We = 2 \frac{\rho_g u_r^2 a}{\sigma}, \quad (2.5)$$

where  $\rho_g$  is the gaseous density,  $u_r$  is the modulus of the relative speed between the droplet and the surrounding air,  $a$  is the droplet radius, and  $\sigma$  is the surface tension coefficient. A larger Weber number implies a more unstable droplet, and the critical number above which breakup will occur (given enough time) can be determined from the empirical relation by Brodkey [9] and also noted by Schmehl *et al.* [47]

$$We_c = 12 (1 + 1.077 Oh^{1.6}), \quad (2.6)$$

where the so-called Ohnesorge number, another dimensionless number, is evaluated as

$$Oh = \frac{\mu_l}{\sqrt{2\rho_l a \sigma}}, \quad (2.7)$$

where  $\mu_l$  is the dynamic viscosity of the liquid. The Ohnesorge number is dependent solely on the droplet itself, whereas the Weber number also includes properties of the surrounding medium and the droplet's relative velocity. We see that the critical Weber number is approximately 12 for droplets with small Ohnesorge numbers,  $\lesssim 10^{-1}$ . For larger value it increases asymptotically as  $Oh^{1.6}$ . It is interesting to study the effect of the droplet diameter on the stability criterion. As it enters the Ohnesorge number in the denominator an increased stability is expected for smaller droplets. The transition where the stability starts to depend on the droplet diameter depends on the other components of the Ohnesorge number; the viscosity, density and surface tension coefficient. In the case of solvent borne clear coat the properties are listed in Table 2.1 where we see that it is the viscosity that stands out the most compared to *e.g.* water. Figure 2.3 shows the

Property	Symbol	Value	Unit
Dynamic viscosity	$\mu$	0.12	$Pa \cdot s$
Density	$\rho$	995	$kg/m^3$
Surface tension	$\sigma$	0.025	$N/m$

Table 2.1: Parameters of the paint material studied: Solvent borne clear coat.

critical Weber number as a function of droplet diameter for the paint material. It is not entirely clear, however, that the scaling is correct for large Ohnesorge numbers as the amount of experimental evidence for  $Oh > 3$  is limited.

The implication by the large Ohnesorge numbers is that the droplets get successively more difficult to break with the scaling  $a^{1.8}$  in the asymptotic limit. More common fluids which are less viscous have only the linear scaling from the Weber number itself.

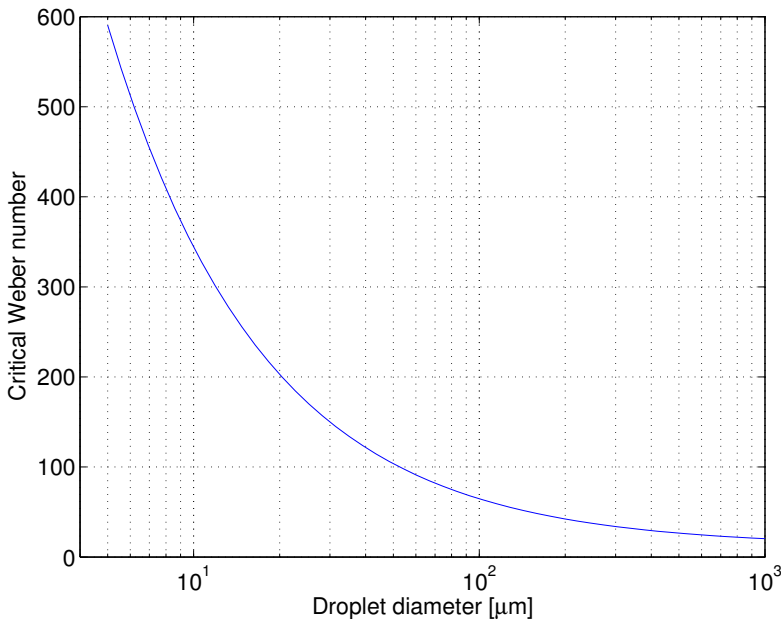


Figure 2.3: Critical Weber number as a function of droplet diameter. Parameters of the paint from Table 2.1.

## 2.4 Numerical modeling

A number of different approaches can be taken when trying to simulate the breakup process. First, a brute-force method could be attempted where each droplet is resolved and all relevant forces are taken into account. Primarily this would be the drag force from the surrounding medium, the internal viscous forces of the droplet, and the surface tension acting on the interface between the droplet and its surroundings. This leads to costly simulations, that also are numerically challenging, as an inherently unstable configuration is being studied. As a spray typically consists of a vast number of droplets, a scaling problem may also arise.

### 2.4.1 Instability theory

A more fruitful approach may therefore be to model the breakup on a higher level. There are a number of fundamental instability mechanisms that can describe the breakup behavior. The most well known ones are probably the Rayleigh-Taylor (R-T) instability, and the Kelvin-Helmholtz (K-H) instability. See the book by Chandrasekhar [12] for a thorough description of instability theory. The R-T instability occurs when two fluids with different densities are accelerated towards each other. An example of a situation where this instability manifests itself is where a denser fluid is placed on top of a less dense fluid. This is an unstable configuration and a tiny disturbance will increase exponentially

in time. The K-H instability is triggered when two fluids are in relative tangential motion. This can be seen as waves on the ocean as the wind blows over the water. These two instabilities have been the foundation for implementation of existing breakup models, see the works by Patterson *et al.* [40], Reitz *et al.* [43], Ricart *et al.* [44], and Su *et al.* [49].

These instabilities govern what happens to a small perturbation of the interface, how fast the disturbance grows and what the unstable wave lengths are. But at some point the disturbance has grown so large that not only a single instability mechanism is active, and subsequently the droplet breaks. If the droplet breaks rapidly such that a single instability can be assumed to be triggered, the knowledge about the instability can be used to model the size and quantity of child droplets after breakup. On the other hand, if the breakup process is slow on a relevant time scale, such that multiple instabilities and strong non-linear behavior are triggered, this is much more difficult. As the breakup in the sprays studied in this work happens at moderate Weber numbers it has been assumed that the breakup is slow, and this modeling technique has not been extensively investigated. It could however be an interesting topic for a future work, especially for a more dilute spray which could more easily be investigated by means of high speed cameras. For the primary breakup it might also prove useful in order to predict the wavelengths present in the filaments spiraling out from the bell edge.

## 2.4.2 TAB model

The Taylor Analogy Breakup (TAB) model [38] has been used in this work to model the breakup of droplets. It is a simplistic method where each droplet is modeled as a one-dimensional harmonic oscillator. The analogy is in that the surface tension is identified as the spring force, the viscosity as the damping, and the relative velocity to the surrounding medium as the driving force. This model does not attempt to describe the breakup in a qualitative way, only quantitatively. The model has a set of parameters that are determined semi-empirically. If the model had been describing the breakup process perfectly, these parameters would have been independent of process conditions and material properties. This cannot be expected from such a simple model, however, and the parameters were optimized to the rotary bell sprayer case in paper III [4]. In addition, the model was modified as described in the paper to include the effect of large viscosity by introducing the Ohnesorge number as described above. This modification does not change the result of the simulation to a large extent, provided that the parameters of the model are re-tuned. This is exactly the point: The parameters of the model should be independent of the process condition and material properties. This modification includes the non-linear effect of viscosity so that the model can be used for fluids of different viscosity without having to re-tune the parameters.

This modification is not the only one that has been attempted on the TAB model. Tanner suggests the Enhanced TAB (ETAB) model [50] where the standard criterion of the TAB model for initiation of a breakup event is kept unmodified, but the resulting child droplet size and velocity distributions are evaluated in a different way. Yeom *et al.* have a similar idea [56] where the child droplets distribution is modified with the total available energy in the parent droplet. Park *et al.* modified the model [39] by including the effect of extra aerodynamic drag on the droplets introduced by the deformation.

Even though all these modifications to the TAB model exist, it still remains a very simple model, but at any rate capable of providing good quantitative results. To give a more qualitative description of the breakup process a model with more degrees of freedom is necessary. One way of realizing that could be to extend the TAB model with higher modes of oscillation. Expanding the droplet in spherical harmonics could be one idea. See the works by Mosler *et al.* [34] and Schmehl [46] for applications of this technique.

The modified TAB model is used in paper III and VI to model the breakup. In the former paper the full droplet size distribution is validated against measurements with good results. In the last paper the spatial distribution of droplets is investigated. As larger droplets carry more momentum and therefore have a larger Stokes number, they are expected to travel in straighter lines and as a consequence appear further away from the bell center than smaller droplets. This hypothesis is verified both experimentally and numerically in the paper. One of the results is reproduced here in Fig. 2.4 where the radial dependency is clearly demonstrated.

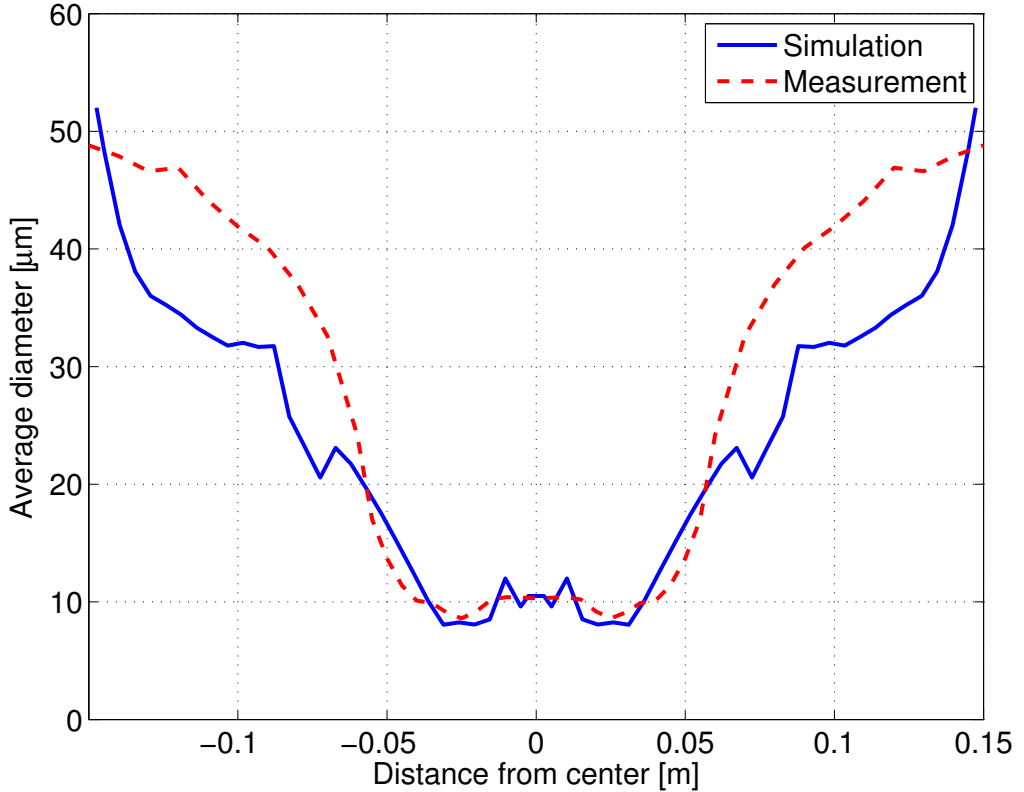


Figure 2.4: Average droplet size distributions as a function of the radial distance from the bell center on a line 50 mm below the bell edge.

# 3 Measurement techniques

Four different measurement techniques have been used in the project: Particle Image Velocimetry (PIV), Phase Doppler Anemometry (PDA), Laser diffraction, and Shadow-graph. In addition, objects of different shapes have been painted and the paint thickness has been measured. Each of these techniques have their strengths and weaknesses, and they are discussed below.

## 3.1 Particle Image Velocimetry (PIV)

This is a technique for measuring particle velocities in a plane. A laser plane is created that illuminates particles within the plane, and a camera directed normally to the plane takes photographs with a suitable time difference in order to record the movement of the particles within the plane. By using two cameras mounted at a slight angle to each other the velocity component out of the plane can also be measured. See Fig. 3.1 for a snapshot taken during PIV measurements.

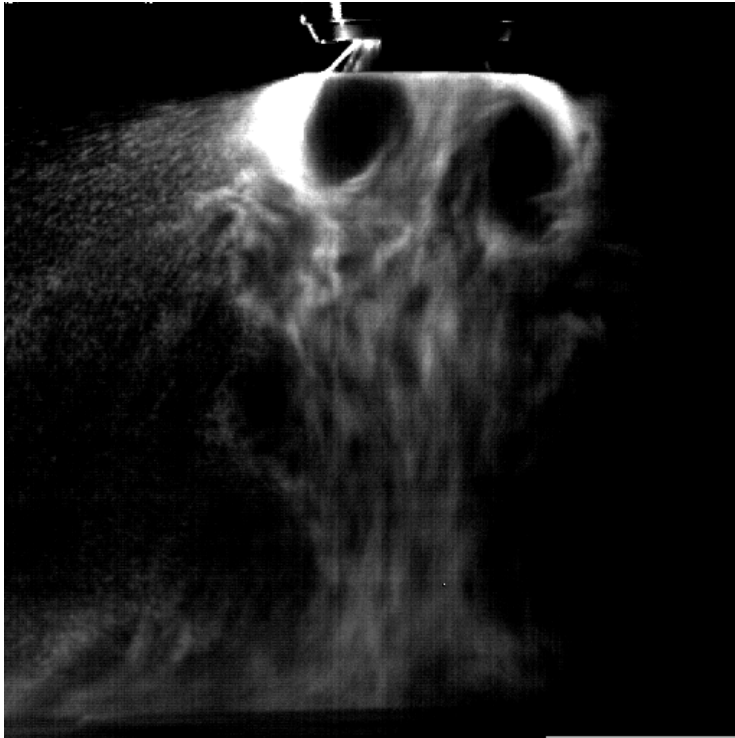


Figure 3.1: PIV snapshot of a bell spraying downwards toward a target. A pair of such images can be used to evaluate the droplet velocities in the plane. Note the two big recirculation regions below the bell.

The technique requires some sort of particles following the flow to be studied. For sprays this is not a problem as droplets are natural particles. If a flow without particles is to be measured a smoke generator could be used for example. See the in-depth paper by Adrian [1] for a description of the technique.

When measuring sprays one has to be aware that it is the droplet speed that is measured. This may, or may not, be the same as the velocity of the background medium depending on the Stokes number. If the range of droplet sizes is very large, ranging from small to large Stokes numbers, the interpretation of the results may be difficult. Note that the technique in itself does not give any information about the droplet sizes.

This measurement technique is not used as a direct basis for any of the appended papers, but the measurements have provided great insights into the fundamental behaviors of the spray application technique studied. In an earlier paper [45] from our group this method was the main experimental technique. Equipment for PIV measurements from LaVision [27], as well as equipment from Dantec Dynamics [13] operated by personnel from Vidix [51], have been used successfully.

## 3.2 Phase Doppler Anemometry (PDA)

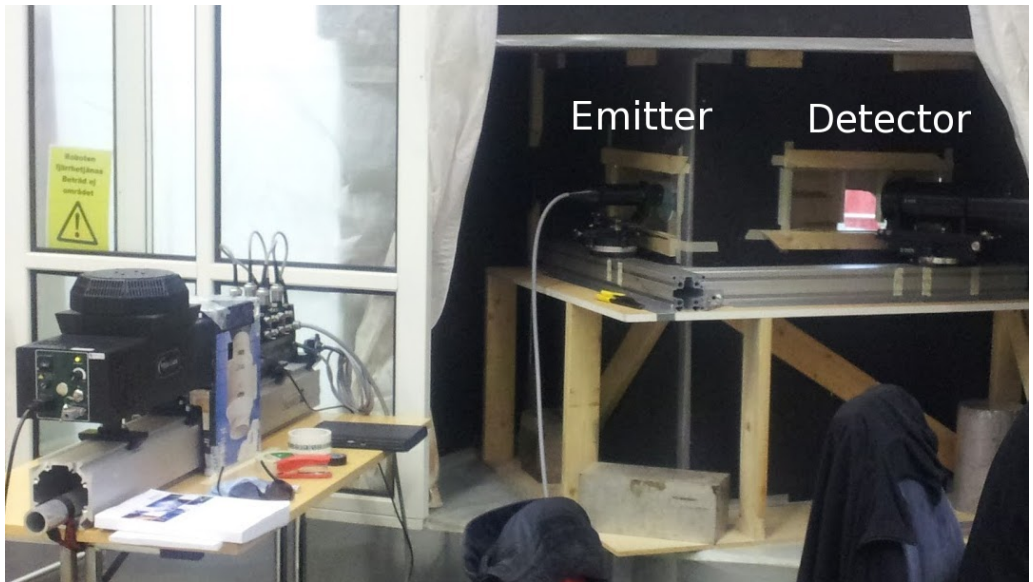
Phase Doppler Anemometry (PDA) is a pointwise measurement technique where single droplets are measured. Both velocity and size information are obtained. Each measurement point is sampled for a number of seconds in order to extract statistical moments such as mean and variance of the droplet sizes and velocities. Some equipments are able to measure two velocity components simultaneously. To measure the remaining component the setup is rotated appropriately. Figure 3.2 shows two photographs from a measurement campaign carried out in October 2012.

As a paint droplet passes through the measurement volume an interference pattern is formed, where the Doppler shift is proportional to the velocity of the droplet. The droplet size is calculated from the phase shift in the signal as detected at different locations at the detector. See [2] for a thorough description of the technique. As the measurements are performed in a very small volume, in practice a point, multiple measurements are typically performed along a line, or even in a plane, in order to obtain spatial information.

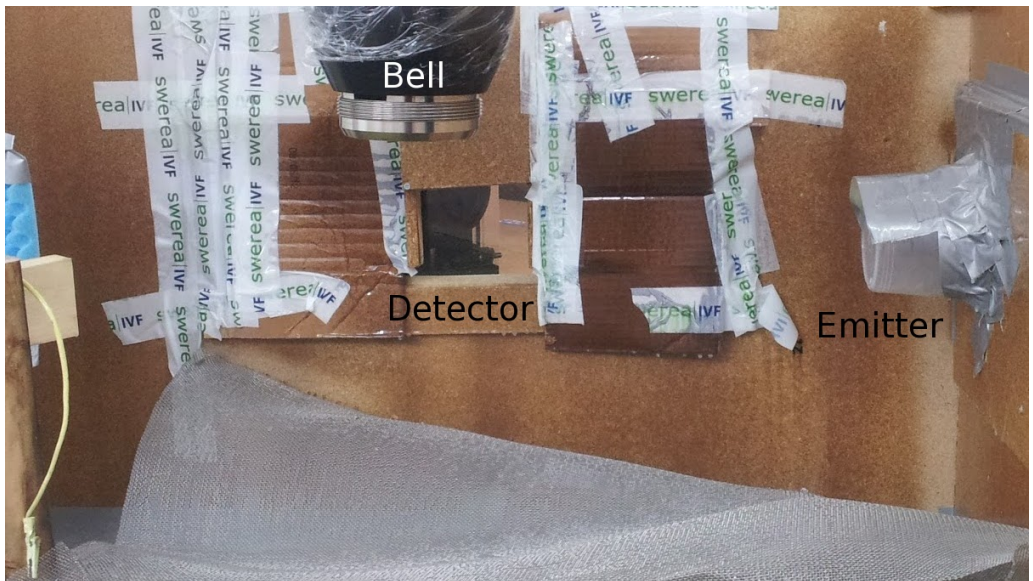
The method was used with equipment from Dantec Dynamics [13] operated by personnel from Vidix [51] to obtain the experimental results in paper VI of this thesis. The ability to measure the spray in a single point formed the basis of the paper.

## 3.3 Laser diffraction

This is a technique for measuring droplet sizes relying on Mie-scattering or Fraunhofer diffraction. Laser light is scattered by the droplets and the scattering angle differs depending on the droplet radius. An array of detectors detecting particles of different size are used to create a histogram of the sizes of droplets present in the spray. See Fig. 3.3 for a photo of an active equipment during a measurement campaign in June 2011. Simmons *et al.* describe the measurement technique in great detail [48].



(a) Front view



(b) Back view

Figure 3.2: Overview of the PDA setup. Four laser beams are emitted and intersect in the measurement point below the bell. The detector is placed appropriately to pick up as much scattered light as possible.



Figure 3.3: Measurement with the laser diffraction technique. A laser beam is emitted from the long tube to the right, diffracted against droplets in the spray, and detected to the left.

Compared to PDA described above this technique does not give any velocity information, only droplet sizes. It measures all particles in a narrow tube and can therefore be said to measure along a line, in contrast to the pointwise measurements of PDA. For the application of rotary bell spray painting, PDA would typically be better suited as it gives the droplet velocities, and can give more localized information. The advantage of the laser diffraction technique is that it gives more information in a single measurement. The global average size distribution can be obtained in a single measurement that takes only about 10 seconds.

Paper III relies on measurements performed with this technique by equipment from Malvern Instruments [28]. The ability to measure the entire spray in a single setup provided an efficient way of obtaining good results.

### 3.4 Shadowgraph

Droplet size information can also be obtained by a technique called shadowgraph. A light source is placed so that it shines directly into a camera with the object of interest

in between. The object will then cast a shadow that is recorded by the camera. The snapshot in Fig. 2.1 is taken with this technique. See also Fig. 3.4 for an example where droplets can be seen. See the book by Merzkirch [32] for an in-depth description of the technique.

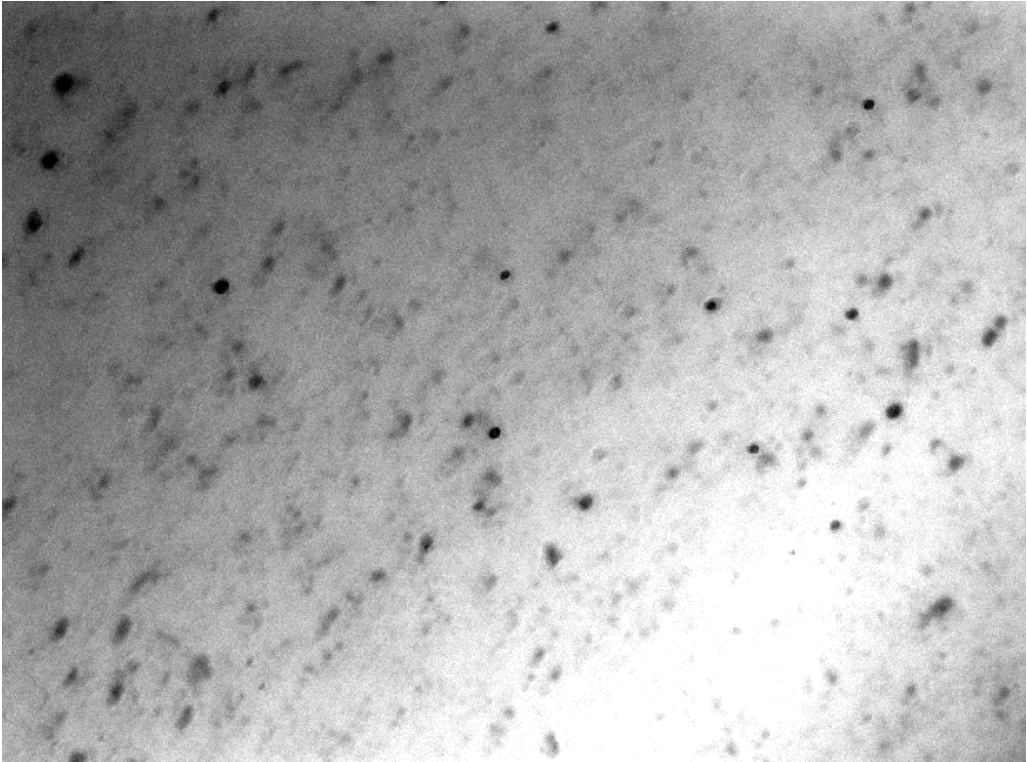


Figure 3.4: A shadowgraph image. Droplets appear as dark shades on a lighter background. As the size of the pixels is known the droplet diameters can be evaluated.

In contrast to the PDA and laser diffraction techniques, but similarly to the PIV measurements, the result of the measurement requires a large amount of post processing where the images are analyzed. To get good averages, a large number of photographs have to be taken at each measurement location, and each of them analyzed. To cover the full spray several locations may have to be measured depending on how large area that is captured by the camera. One also has to be careful about the resolution in the pictures, as it is theoretically impossible to estimate the diameter of a droplet casting a shadow on a single pixel or less in the camera. In practice about ten pixels over the diameter is the lower limit. This condition makes the technique less suitable for measurements of the types of sprays studied here. As the spray cones are relatively large, the camera needs to be far away from the measurement zone, and this limits the resolution. On the other hand, for investigating the filaments as shown in Fig. 2.1 it is a very good technique as these are

relatively large, and the fact that no assumptions on the shape of the objects are made during the measurement phase. Once the pictures are taken, image analysis methods can be implemented to extract information from the photographs. This technique may also give in-plane velocities if photos are taken with a suitable, well known, time difference as the movement between two subsequent photos can be evaluated.

None of the appended papers relies directly on measurements made with this technique. It is not as suited for the sprays studied in this work as the previously mentioned PDA and laser diffraction methods. It is, however, very well suited for studying the primary breakup region. If this region of the flow had been studied the method would have provided high quality measurements. The measurements have also provided great insights into the flow behavior close to the bell edge. Equipment from LaVision [27], as well as equipment from Dantec Dynamics [13] operated by personnel from Vidix [51], have been used for measurements with the shadowgraph technique.

# 4 High performance computing

At some point in projects dealing with development of software for simulations, not only the accuracy and flexibility are important, but also the computational performance needs improvement. It could either be the speed of the simulation, its size, or even both. There are a number of things that can be done to increase the performance. The algorithm is of course of utmost importance. It does not matter how clever the programmer is if the implemented algorithm is not suited to the task. This is therefore probably the most important point to consider. Next could be the programming language. Here there is usually a trade-off between programming time and running time. Programming languages that give a lot of freedom to utilize the hardware to its full potential are usually harder to program in. This is becoming less of an issue with modern programming languages and compilers. There are now very few people that program assembler more efficiently than what a modern C or Fortran compiler generates, on a reasonably sized computational task. Furthermore, the time required to write and fine-tune the assembly code is very large, so that this is not a reasonable alternative anymore.

Modern hardware now has a number of computational cores, ranging from 4 to about 16 per processor. This can also be doubled by different solutions where the same physical hardware unit presents itself as two units to the operating system. Intel calls this Hyper-Threading and can give a significant improvement for some type of tasks. On the other hand, it may also give a slight performance degradation on other workloads. Therefore, the programmer needs to make use of the available hardware in an efficient way.

## 4.1 Parallelization

Parallelization of a program can give a great boost in the performance. By including cache-effects the speedup may even be super-linear if the programmer is skillful and the algorithm makes full use of the hardware. This is of course often not the case, for different reasons. The algorithm may require some synchronization points, or a different part of the hardware becomes the bottleneck. This could be the communication links between computational units, or the memory bus for accessing the RAM, which usually does not scale well on current hardware.

What needs to be taken into consideration, however, is that not all algorithms are suited to be parallelized, or may only scale up to a small number of threads. One therefore has to be careful when evaluating the performance of a parallel program. A very good serial algorithm may outperform the best parallel one for a given task even for a relatively large number of threads executing the parallel algorithm. It may therefore not be fair to compare the same algorithm running on different number of threads, as a different algorithm may perform better for a small, or very large, number of threads.

### 4.1.1 Shared memory parallelization

When parallelizing on a shared memory computer all of the memory space can be read and written by all of the threads. This is of course very convenient, but may also be a

source of bugs known as race conditions where one thread reads a piece of memory and another thread writes to it at the same time. It is therefore very important to keep track of which dependencies exist on the data between different threads.

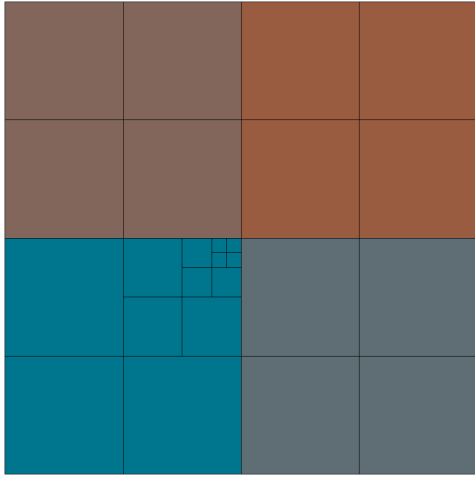
Currently no good tools exist for automatic parallelization of C or C++ code. OpenMP [37] is perhaps the most generally used toolkit for scientific code. To parallelize a simple `for loop`, for example, is trivial provided that each iteration in the loop is independent of all the other. To obtain maximum efficiency it gets more tricky, however, as one needs to take into consideration the memory layout and cache effects and things like that. This technique of parallelizing programs is used to varying degrees in all papers of this thesis.

Recently, the trend in parallelization is to create tasking models. That is, the problem at hand is divided into a number of tasks with well defined dependencies. The execution environment then performs the tasks in such an order that all preconditions are met. The theory is that it always exist enough tasks that are able to be computed such that the processor can be kept fully occupied at all times. This is a promising technique that may become more widely used over the coming years.

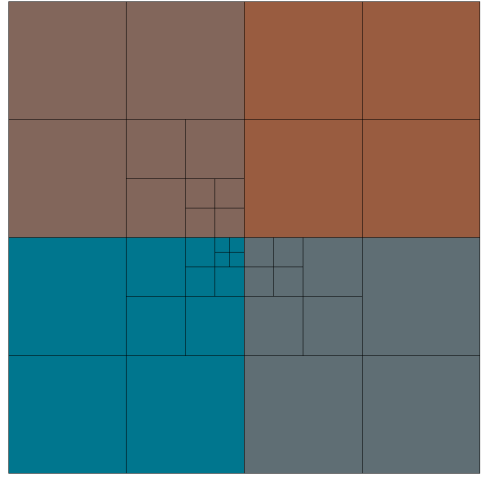
### 4.1.2 Message passing

If not all memory is accessible by all parts of the program a message passing technique is often used, such as MPI [35]. Compared to a shared memory parallelization an MPI program is much more complicated to write. It has a much greater potential of achieving high performance, however, as more computers may be connected together in a cluster. In a simple form this could be a number of standard desktop computers connected over a network where all the computers, or nodes, execute the same program and are communicating over the network. The challenge here is to balance the workload so that all nodes are fully occupied at all times. Communication is also usually slow compared to carrying out computations and should therefore be minimized. If possible, the communication should be carried out in parallel with the computations so that when a computational task is completed the next has already been prepared in the communication step and can be executed immediately after the previous task is completed. This adds an additional complexity level to the program, but is often necessary in order to achieve maximum performance.

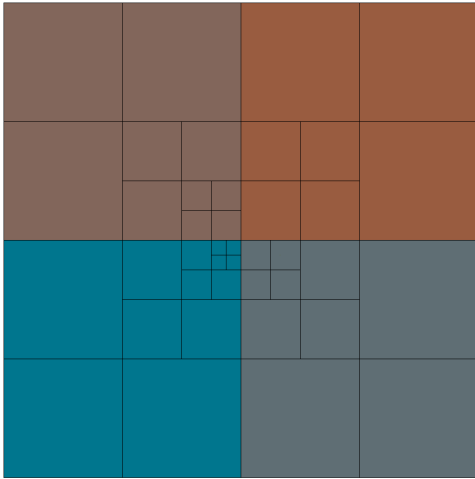
As the communication is much more complicated compared to a shared memory parallelization the choice of algorithm is even more limited. On the other hand, by having access to more hardware, larger simulations that do not fit into the memory of a single computer can be performed. Paper IV describes the parallelization of an existing implementation of the Navier-Stokes solver IBOFlow [21] using this technique. As the octree grid generator is an integrated part of the solver it is also parallelized. The computational grid has to obey certain rules to be a valid grid for the solver. One such rule is that neighboring cells must not differ in size more than a factor of two. As the grid consists of Cartesian cells this is easily implemented in the serial version of the grid generator, but is more demanding when done in parallel. To solve the issue an iterative loop is applied where neighboring blocks of cells are updated to obey the rule. See Fig. 4.1 for a sequence of generated grids, where the final grid complies with the rules.



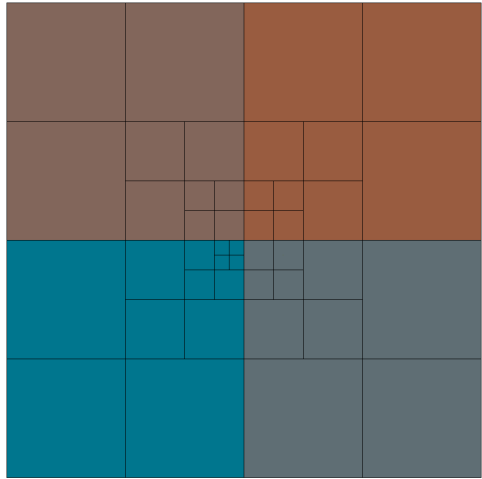
(a) The upper right corner of the lower left block has been refined three times.



(b) The upper left and lower right block has been refined as a consequence of the balancing rule.



(c) The upper right block has been refined once.



(d) The upper right block has been refined twice fulfilling the grid rules also on the diagonal.

Figure 4.1: The different stages of grid balancing.

More details of the implementation including its scaling properties can be found in the paper.

## 4.2 Accelerators

In the last few years there has been a trend to use so-called accelerators to carry out computations. The most common type of accelerator is a graphics card which has been extended to carry general purpose computations, as General Purpose Graphics Processing Unit (GPGPU). The major benefits of these cards are a large number of computational cores (in the order of thousands), and a larger memory bandwidth compared to the conventional RAM. The disadvantage is the cost of transferring data back and forth to the card, and that the computational cores are not very powerful individually. Smaller groups of cores also execute the exact same code simultaneously, but with different input data, so-called SIMD (single instruction, multiple data) execution. To gain the most out of these cards one therefore has to minimize the communication with the card, and have an algorithm that is well suited for massive parallelization. BLAS (Basic Linear Algebra Subprogram) routines are of this type, and iterative solvers such as Conjugate Gradient (CG) and Generalized Minimal Residual (GMRES) can therefore be very efficient on this type of hardware. On the other hand, no competitive implementation of an algebraic multigrid solver is currently available, as this algorithm is not very well suited for massive parallelization of SIMD type.

Because of the characteristics of doing specific things very fast, and others prohibitively slow, it is very important to think carefully about which tasks should be executed on the graphics card. As discussed above, one also has to be careful when comparing the CPU performance to the GPGPU's. For example, solving a sparse linear system of equations as appearing from the Laplace operator with the CG method is typically much faster on the GPGPU than on the CPU due to the superior memory bandwidth on the accelerator. To be fair, the transfer cost of the matrix and right hand side and solution vectors should probably be included in the total time for solving on the GPGPU, unless a larger part of the program is actually running on it and transfer to the CPU is not necessary. But by solving the system of equations with an efficient algebraic multigrid method the CPU can become competitive again, especially for larger system sizes. In practice the GPGPUs currently appear to be most beneficial for intermediate system sizes,  $10^4 \lesssim N \lesssim 10^6$ , where  $N$  is the number of unknowns. An Nvidia GeForce GTX 560 Ti graphics processor was used in simulations performed in paper III.

Within the spray painting project a Navier-Stokes solver was implemented to run exclusively on the GPGPU as a Master Thesis project by Karlsson [26]. By implementing the full solver to be executed on the accelerator the cost of sending data between the CPU and GPGPU is avoided. As noted above, care has to be taken to make sure that all parts of the solver are parallelized, however, as the GPGPU does not perform well on serial tasks. By doing this Karlsson reports speedups of a factor 15.5 compared to an OpenMP-parallel implementation running on the CPU, in the case when both programs use the iterative CG and GMRES methods for solving the equations. See Fig. 4.2 where the speedup is given for a number of different grid sizes. This promising result is however reduced to a more moderate speedup of 2.0 when using a more efficient Algebraic Multigrid method on the CPU. As noted above, this method is not suited for implementing on the GPGPU. It remains to be seen if someone manages this in the future.

A factor of two is definitely not bad, and the potential of GPGPUs to accelerate

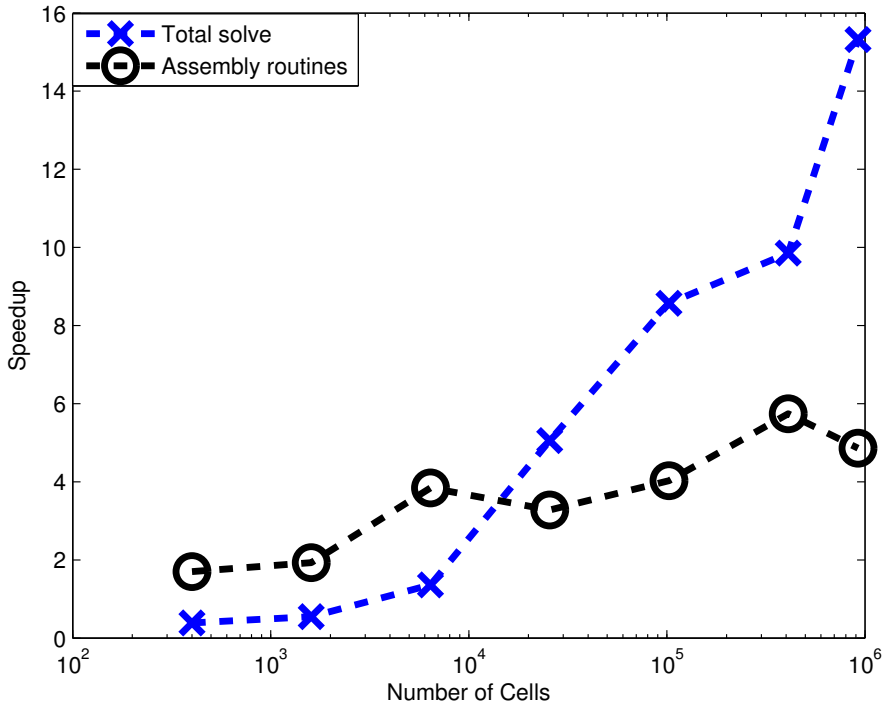


Figure 4.2: Speedup of a GPGPU implementation of the Navier-Stokes equations compared to an OpenMP-parallel implementation on the CPU. Reproduced with permission from N. Karlsson [26].

simulation software should not be ignored. Two main limiting factors can currently be identified: The more complicated programming of GPGPUs and relative lack of standardized programming languages, and the limited amount of memory available on a single GPGPU. Currently 2 – 3 GiB of on-chip RAM is available on common consumer-level cards, which implies that Navier-Stokes simulations with up to a few million degrees of freedom can be performed.



## 5 Summary of appended papers

### 5.1 Paper I — Simulation of Electrostatic Rotary Bell Spray Painting in Automotive Paint Shops

The paper describes the software and the numerical methods used to simulate the spray painting of complex objects. The equations governing the gaseous phase and the Lagrangian particles are presented and their solutions are discussed. Immersed boundary techniques are used to enforce the boundary conditions on the internal interfaces of the spray paint applicator and the target to be painted.

The complex multiphysics nature of the spray painting is discussed and a framework of coupled equations is proposed. The fluid velocity, electrostatic potential, and paint droplets all interact, creating a large coupled simulation. Efficient solvers for all parts are described and the coupling between them discussed.

Flat plates as well as a more complicated geometric shape in form of a car front fender are measured and simulated with several process conditions and robot paths. Good agreement is demonstrated in all cases, including at the edges and concave parts on the fender where the electrostatic effect is an important factor.

### 5.2 Paper II — Modeling Surface Tension in SPH by Interface Reconstruction using Radial Basis Functions

The paper describes a novel discretization of the surface tension force associated with interfaces between fluids. It is a force that is inversely proportional to the size of the object it is acting on, and at some point it therefore becomes the dominant force, balanced mostly by the pressure gradient. A force of this magnitude is crucial to discretize in an appropriate way as small errors may render the simulation oscillative and unstable.

The contribution describes a way of creating a smooth force field by reconstructing the interface between the fluids in a grid-independent manner. It does so by means of Radial Basis Functions [55, 10, 11] with the approximation feature described in [24]. By introducing the  $\eta$  parameter ranging from 0 to 1 the smoothness of the approximation can be tuned to an appropriate level. In the limit of no additional smoothing the approximation turns into an interpolation of the interface that typically varies on the length scale of the computational grid. By adding some smoothing this grid dependence is removed and non-physical locally concave parts of the interface are removed.

The model is validated using two standard test cases for surface tension: The time period of the oscillations of an ellipsoid subject to surface tension, and Laplace's law which relates the pressure drop over the interface to its curvature. Both cases show good results and highlights the ability to create stable simulations over long times, without having non-physical disturbances of the velocity field.

## 5.3 Paper III — A Modified TAB Model for Simulation of Atomization in Rotary Bell Spray Painting

The paper describes the application of the Taylor Analogy Breakup (TAB) model [38] to the rotary bell spray painting case. The properties of the paint material differ from what the TAB model has been used for traditionally. In particular, the viscosity of the paint is approximately 100 times that of water. For this reason a correction for large viscosity originally described by Brodkey [9] is applied to the TAB model.

The breakup consists of two phases, primary and secondary breakup, of which only the secondary breakup is treated by the TAB model. The primary breakup is defined as the breakup of the filaments of paint emanating from the edge of the bell as it rotates. The filaments extend a few millimeters away from the edge and are then broken up into non-spherical droplets. The size distribution of these initial fragments are modeled by a log-normal distribution of relatively large droplets that are to a large degree broken once more by the TAB model in the secondary phase. The speed of the fragments is modeled by a uniform distribution ranging from the tangential velocity of the bell to half of it.

As the application is new to the model its parameters need to be tuned such that the simulated droplet size distributions match measured ones. The global optimization algorithm DIRECT [25] was used to this purpose. One of the five parameters of the model was found to not affect the obtained size distributions and the optimization was reduced to four free variables. Three different rotation speeds were considered: 30, 40, and 50 thousand revolutions per minute (RPM). By optimizing against all the three cases simultaneously a good agreement over the full range was obtained.

## 5.4 Paper IV — MPI-Parallelization of a Structured Grid CFD Solver including an Integrated Octree Grid Generator

An existing Computational Fluid Dynamics (CFD) solver is parallelized by means of MPI. The solver includes a dynamic and adaptive grid generator for Cartesian Quadtree and Octree grids, which therefore also has to be parallelized. The grid generator generates grids fulfilling a specific set of rules that have to be enforced also in parallel, complicating the matter substantially.

The assembly of the large sparse matrices resulting from the implicit discretization of Navier-Stokes equations is done in parallel, as is the solving process. The parallel performance of both of these processes depends heavily on a good load balancing in order to reach satisfactory speedup. Two versions of load balancing are demonstrated, one based on block swapping, and the other by utilizing the Metis or Parmetis software packages for load balancing of graphs. The performance is analyzed and good results are demonstrated.

The solvers AGMG [36] and Hypre [17] are demonstrated to scale very well with the number of processors, even though Hypre is a bit too slow for practical use. The AGMG

solver is very fast on the other hand, giving affordable solution times for the largest cases of 50 million cells considered.

## 5.5 Paper V — Modeling Surface Tension by Interface Reconstruction using Radial Basis Functions

The paper is an extension of paper II, where the discretization of the surface tension is integrated in the Volume of Fluids (VoF) method [19] as opposed to the Smoothed Particle Hydrodynamics (SPH) method [33]. Improvements to the discretization is made such that the  $\eta$  parameter is made independent of the size and grid resolution of the simulated droplet.

Two standard validation cases are shown: The time period of the oscillations of an ellipsoid subject to surface tension, and Laplace’s law which relates the pressure drop over the interface to the its curvature, and both cases show good results. A grid study is performed on the latter case, where first order accuracy in the grid size is demonstrated. A comparison to the standard CSF method [8] of discretizing the surface tension is made, where it is seen that the proposed method gives a much smoother force field, and that it also has better grid convergence properties.

## 5.6 Paper VI — Modeling and Simulation of Droplet Breakup in Automotive Spray Painting

Detailed simulations of the near bell region of rotary bell spray painting are presented in this paper. By including the bell geometry in the simulations and by simulating the conditions for paint and shape air injection, detailed knowledge about the paint droplet trajectories immediately after injection is gained. Large droplets carrying more momentum typically travel in wider trajectories from the bell edge towards the target compared to smaller droplets. This can be seen in the local droplet size distributions where the mean size increases with the distance to the center.

Phase Doppler Anemometry (PDA) is used to measure the flow conditions, including local droplet size distributions, along two lines below the bell. The Taylor Analogy Breakup (TAB) model with the modification described in paper III is used to model the breakup of the paint droplets. The turbulence is modeled by the one-equation Spalart-Allmaras DES model.

Two different cases are presented, a stationary bell, and a stroke over a plate. In the former case, size distributions and droplet densities along two different lines below the bell are compared to measurements. Averages are taken over time, but also in the azimuthal direction due to the symmetric configuration of the bell. In the stroke case, the film build on the plate is compared to the result of physical painting. Both cases show good agreement with measurements.



## 6 Summary and future work

The work in this thesis targets the region close to a rotary bell sprayer and attempts to explain the complicated processes taking place there. Papers III and VI focus on what happens to the paint droplets after injection, and, in particular, their final sizes. The TAB model is successfully capturing the droplet size distribution, both in a global sense, as well as the spatial variations below the bell. To extract even more information about the droplets and the air flow close to the bell a better suited mesh that is not isotropically refined would be greatly beneficial. As the configuration is cylindrically symmetric a small sector could even be simulated in great detail. This would require some thought when it comes to boundary conditions, however, since it is not an instantaneously stationary process.

Papers II and V deal with fundamental numerical aspects of how to discretize the surface tension force acting on a droplet. This force is numerically very sensitive and unstable in its nature, and it is therefore important to have a very good discretization. The derived surface tension discretization could as an application be used to simulate droplet breakup, or the breakup of the filaments spiraling out from the bell edge. The latter is a subject that deserves more investigation. One, or both, of two main routes should probably be taken: direct numerical simulation of the two interacting phases, or the more analytical approach of instability analysis. The situation close to the bell edge is relatively idealized, in some sense, such that not too crude approximations have to be applied in order to give an analytical description of the phenomena. As long as two filaments do not interact this should be a viable approach. If direct numerical simulations are to be performed a parallel software of the type described in paper IV is definitely needed.

The novel surface discretization described does not account for wall contacts in any form. This would be an obvious extension of the work. In principle, the method should be very well suited for including wall contact, as it relies on a reconstructed implicit surface. It is therefore only a matter of setting the correct boundary conditions for the implicit surface at the contact point. In this way arbitrary contact angles should be straight forward to handle. In practice, however, this require some thought on how it should be included in the interpolation problem in a mathematically and numerically sound way.

Electrostatic forces among the paint droplets are not considered in this work. They have two main effects: aiding the atomization, and the pairwise repulsion between droplets. The former effect should be straight forward to include in the breakup models as the charges act as a negative surface tension. That is, charges are located at the surface of the droplet, and the charges repel each other. If enough charges are present on a single droplet the Rayleigh limit [42] is reached and the droplet breaks. To investigate this effect some experimental support would be needed. The second effect, electrostatic repulsion between droplets, could also be investigated. Experimental evidence show that this causes a macroscopic effect where the spray pattern is widened, and that the local fluctuations of droplet number density is reduced. This effect is therefore also relevant on the larger scale of simulations as performed in paper I.

Highly detailed simulations of the near bell region could serve as an alternative to

cumbersome and expensive measurements. By sampling the detailed simulations below the bell edge information can be gained on how the setup a simulation of the type presented in paper I. Once the paint has broken up into small stable droplets, it drastically slows down and assumes the local air flow speed within a very short distance. As the flow settles and the large gradients disappear much faster simulations with more moderate demands on cell sizes can be created where the painting of complex geometries is feasible.

# References

- [1] R. J. Adrian. Particle-Imaging Techniques for Experimental Fluid Mechanics. *Annual Review of Fluid Mechanics* **23.1** (1991), 261–304.
- [2] H. Albrecht. *Laser Doppler and Phase Doppler Measurement Techniques*. Engineering Online Library. Springer, 2003.
- [3] B. Andersson, A. Ålund, A. Mark, and F. Edelvik. *MPI-Parallelization of a Structured Grid CFD Solver including an Integrated Octree Grid Generator*. Tech. rep. 2013-05. Chalmers University of Technology, Sept. 2013.
- [4] B. Andersson, V. Golovitchev, S. Jakobsson, A. Mark, F. Edelvik, L. Davidson, and J. S. Carlson. A Modified TAB Model for Simulation of Atomization in Rotary Bell Spray Painting. *Journal of Mechanical Engineering and Automation* **3.2** (2013), 54–61.
- [5] B. Andersson, S. Jakobsson, A. Mark, F. Edelvik, and L. Davidson. “Modeling Surface Tension by Interface Reconstruction using Radial Basis Functions”. Submitted to *Journal of Multiphase Flow*.
- [6] B. Andersson, S. Jakobsson, A. Mark, F. Edelvik, and L. Davidson. “Modeling Surface Tension in SPH by Interface Reconstruction using Radial Basis Functions”. *Proceedings of the 5<sup>th</sup> International SPHERIC Workshop*. Ed. by B.D. Rogers. Manchester (U.K.), June 2010, pp. 7–14.
- [7] B. Andersson, A. Mark, L. Davidson, F. Edelvik, and J. Carlson. “Modeling and Simulation of Droplet Breakup in Automotive Spray Painting”. To be submitted for journal publication.
- [8] J. U. Brackbill, D. B. Kothe, and C. Zemach. A continuum method for modeling surface tension. *Journal of Computational Physics* **100.2** (1992), 335–354.
- [9] R. S. Brodkey. *The Phenomena of Fluid Motions*. Addison-Wesley Series in Chemical Engineering. New York, NY, USA: Addison-Wesley Pub. Co., 1967.
- [10] M. D. Buhmann. “Radial basis functions”. *Acta numerica, 2000*. Vol. 9. Acta Numer. Cambridge: Cambridge Univ. Press, 2000, pp. 1–38.
- [11] M. D. Buhmann. *Radial basis functions: theory and implementations*. Vol. 12. Cambridge Monographs on Applied and Computational Mathematics. Cambridge: Cambridge University Press, 2003.
- [12] S. Chandrasekhar. *Hydrodynamic and Hydromagnetic Stability*. Dover Books on Physics Series. Dover Publications, 1961.
- [13] *Dantec Dynamics*. <http://www.dantecdynamics.com>.
- [14] J. Domnick, A. Scheibe, and Q. Ye. The Simulation of Electrostatic Spray Painting Process with High-Speed Rotary Bell Atomizers. Part II: External Charging. *Particle & Particle Systems Characterization* **23.5** (2006), 408–416.
- [15] J. Domnick, A. Scheibe, and Q. Ye. The Simulation of the Electrostatic Spray Painting Process with High-Speed Rotary Bell Atomizers. Part I: Direct Charging. *Particle & Particle Systems Characterization* **22.2** (2005), 141–150.
- [16] K. R. Ellwood and J. Braslaw. A finite-element model for an electrostatic bell sprayer. *Journal of Electrostatics* **45.1** (1998), 1–23.
- [17] R. Falgout. *Hypre Linear Algebra Solver Package*.

- [18] R. Goldman. Curvature formulas for implicit curves and surfaces. *Computer Aided Geometric Design* **22.7** (2005). Geometric Modelling and Differential Geometry, 632–658.
- [19] C. Hirt and B. Nichols. Volume of fluid (VOF) method for the dynamics of free boundaries. *Journal of Computational Physics* **39.1** (1981), 201–225.
- [20] H. Huang, M. Lai, and W. Meredith. “Simulation of spray transport from rotary cup atomizer using KIVA-3V”. *10<sup>th</sup> International KIVA User’s Group Meeting*. Detroit, MI, USA, 2000.
- [21] *IBOFlow*. <http://www.iboflow.se>.
- [22] K. Im, R. Matheson, M. Lai, and S. Yu. Simulation of Spray Transfer Processes in Electrostatic Rotary Bell Sprayer. *Journal of Fluids Engineering* **126.3** (2004), 449–456.
- [23] *IPS Virtual Paint*. <http://www.industrialpathsolutions.com>.
- [24] S. Jakobsson, M. Patriksson, J. Rudholm, and A. Wojciechowski. A method for simulation based optimization using radial basis functions. *Optimization and Engineering* **11** (4 2010), 501–532.
- [25] D. R. Jones, C. D. Perttunen, and B. E. Stuckman. Lipschitzian optimization without the Lipschitz constant. *J. Optim. Theory Appl.* **79** (1 Oct. 1993), 157–181.
- [26] N. Karlsson. “An Incompressible Navier-Stokes Equations Solver on the GPU Using CUDA”. Master’s Thesis. Chalmers University of Technology, 2013.
- [27] *LaVision*. <http://www.lavision.de/en>.
- [28] *Malvern Instruments*. <http://www.malvern.com>.
- [29] A. Mark, B. Andersson, S. Tafuri, K. Engström, H. Söröd, F. Edelvik, and J. S. Carlson. Simulation of Electrostatic Rotary Bell Spray Painting in Automotive Paint Shops. *Atomization and Sprays* **23.1** (2013), 25–45.
- [30] A. Mark, R. Rundqvist, and F. Edelvik. Comparison Between Different Immersed Boundary Conditions for Simulation of Complex Fluid Flows. *Fluid Dynamics & Materials Processing* **7.3** (2011), 241–258.
- [31] A. Mark and B. van Wachem. Derivation and validation of a novel implicit second-order accurate immersed boundary method. *Journal of Computational Physics* **227.13** (2008), 6660–6680.
- [32] W. Merzkirch. *Flow visualization*. Second edition. New York: Academic Press, 1987.
- [33] J. J. Monaghan. Smoothed particle hydrodynamics. *Reports on Progress in Physics* **68.8** (2005), 1703.
- [34] A. B. Mosler and E. S. G. Shaqfeh. Drop breakup in the flow through fixed beds via stochastic simulation in model Gaussian fields. *Physics of Fluids* **9.11** (1997), 3209–3226.
- [35] MPI Forum. *MPI: A Message-Passing Interface Standard. Version 2.2*. Sept. 2009.
- [36] Y. Notay. *An aggregation-based algebraic multigrid method*. Tech. rep. GANMN 08-02. Brussels, Belgium: Universite Libre de Bruxelles, 2008 (revised 2009).
- [37] OpenMP Architecture Review Board. *OpenMP Application Program Interface Version 3.0*. May 2008.
- [38] P. O’Rourke and A. Amsden. The TAB method for numerical calculation of spray droplet breakup. *SAE paper 872089* (1987).

- [39] J.-H. Park, Y. Yoon, and S.-S. Hwang. Improved TAB Model for Prediction of Spray Droplet Deformation and Breakup. *Atomization and Sprays* **12.4** (2002), 387–401.
- [40] M. Patterson and R. Reitz. Modelling the effects of fuel spray characteristics on Diesel engine combustion and emission. *SAE paper 980131* (1998).
- [41] M. Pilch and C. Erdman. Use of breakup time data and velocity history data to predict the maximum size of stable fragments for acceleration-induced breakup of a liquid drop. *International Journal of Multiphase Flow* **13.6** (1987), 741–757.
- [42] L. Rayleigh. On the equilibrium of liquid conducting masses charged with electricity. *Philosophical Magazine Series 5* **14.87** (1882), 184–186.
- [43] R. Reitz. Modeling Atomization Processes in High-Pressure Vaporizing Sprays. *Atomization and Spray Technology* **3** (1987), 309–337.
- [44] L. Ricart, J. Xin, G. Bower, and R. Reitz. In-Cylinder Measurement and Modeling of Liquid Fuel Penetration in a Heavy-Duty Diesel Engine. *SAE paper 971591* (1997).
- [45] R. Rundqvist, A. Mark, B. Andersson, A. Ålund, F. Edelvik, S. Tafuri, and J. Carlsson. “Simulation of Spray Painting in Automotive Industry”. *Numerical Mathematics and Advanced Applications 2009*. Ed. by G. Kreiss, P. Lötstedt, A. Målqvist, and M. Neytcheva. Springer Berlin Heidelberg, 2010, pp. 771–779.
- [46] R. Schmehl. “Advanced Modeling of Droplet Deformation and Breakup for CFD Analysis of Mixture Preparation”. *Proceedings of the 18<sup>th</sup> Annual Conference on Liquid Atomization and Spray Systems*. Zaragoza, Spain, Sept. 2002.
- [47] R. Schmehl, G. Maier, and S. Wittig. “CFD Analysis of Fuel Atomization, Secondary Droplet Breakup and Spray Dispersion in the Premix Duct of a LPP Combustor”. *Eighth International Conference on Liquid Atomization and Spray Systems*. Pasadena, CA, USA, July 2000.
- [48] M. J. Simmons and T. J. Hanratty. Droplet size measurements in horizontal annular gas–liquid flow. *International Journal of Multiphase Flow* **27.5** (2001), 861–883.
- [49] T. Su, M. Patterson, R. Reitz, and P. Farrell. Experimental and Numerical Studies of High Pressure Multiple Injection Sprays. *SAE paper 90861* (1996).
- [50] F. X. Tanner. Liquid Jet Atomization and Droplet Breakup Modeling of Non-Evaporating Diesel Fuel Sprays. *SAE paper 970050* (1997).
- [51] VIDIX - Visible Dynamics AB. <http://www.vidix.se>.
- [52] V. Viti, J. Kulkarni, and W. A. “CFD Analysis of the Electrostatic Spray Painting Process”. *21<sup>th</sup> Annual Conference on Liquid Atomization and Spray Systems*. Orlando, FL, USA, May 2008.
- [53] V. Viti, A. Salazar, and S. Saito. Numerical Study of the Coupling between the Flowfield and the Electrostatic Field inside an Automotive Spray Paint Booth. *Transactions of the IASME* **2.2** (2005), 261–269.
- [54] J. A. Walton. Surface tension and capillary rise. *Physics Education* **7.8** (1972), 491–498.
- [55] H. Wendland. *Scattered data approximation*. Vol. 17. Cambridge Monographs on Applied and Computational Mathematics. Cambridge: Cambridge University Press, 2005.
- [56] J.-K. Yeom, M.-J. Lee, S.-S. Chung, J.-Y. Ha, J. Senda, and H. Fujimoto. A proposal for diesel spray model using a TAB breakup model and discrete vortex method. *KSME International Journal* **16.4** (2002), 532–548.

- [57] Q. Ye, B. Shen, O. Tiedje, and J. Domnick. “Investigations of spray painting processes using an airless spray gun”. *24<sup>th</sup> European Conf. on Liquid Atomization and Spray Systems*. Estoril, Portugal, 2011.